Fatigue Life Methodology for Bonded Composite Skin/Stringer Configurations

Ronald Krueger, Isabelle L. Paris*, and T. Kevin O'Brien***

*National Research Council Research Asscociate

**U.S. Army Research Laboratory, Vehicle Technology Directorate

NASA Langley Research Center, Hampton, Virginia

Pierre J. Minguet

The Boeing Company, Philadelphia, Pennsylvania

ABSTRACT

A methodology is presented for determining the fatigue life of bonded composite skin/stringer structures based on delamination fatigue characterization data and geometric nonlinear finite element analyses. Results were compared to fatigue tests on stringer flange/skin specimens to verify the approach.

INTRODUCTION[1]

Many composite components in aerospace structures are made of flat or curved panels with co-cured or adhesively bonded frames and stiffeners. Testing of stiffened panels designed for pressurized aircraft fuselage has shown that bond failure at the tip of the frame flange is an important and very likely failure mode. Comparatively simple specimens consisting of a stringer flange bonded onto a skin were developed [1-3]. The failure that initiates at the tip of the flange in these specimens is identical to the failure observed in the full-scale panels and the frame pull-off specimens.

The first objective of this work was to investigate the damage mechanisms in bonded composite skin/stringer specimen under tension fatigue loading conditions. Microscopic investigations of the specimen edges were used to document the onset of matrix cracking and delamination as a function of fatigue cycles and to identify typical damage patterns.

The second objective of this work was to develop an analytical methodology to accurately predict the onset of matrix cracking and delamination. The tension loading was simulated in a geometrically nonlinear analysis using a two-dimensional plane-stress finite element model. A stress analysis was used to predict the location and orientation of the first transverse crack based on the principal transverse tension stress distribution in the flange tip area. A fracture mechanics approach was used to determine delamination onset from this transverse crack.

---

[1] In Proceedings of the American Society for Composites, Fifteenth Technical Conference, Technomic Publishing, ISBN 1-58716-053-6, pp. 729-736, 2000.

MATERIALS AND SPECIMEN PREPARATION

The specimens consisted of a tapered flange, representing the stringer, bonded onto a skin (Figure 1). An IM7/8552 graphite/epoxy system was used for skin and flange. The skin lay-up was [45/-45/0/-45/45/90/90/-45/45/0/45/-45] using prepreg tape. The flange was made of a plain-weave fabric, and the lay-up was $[45/0/45/0/45/0/45/0/45]_f$, where 0 represents a 0°-90° fabric ply and 45 represents a 0°-90° fabric ply rotated 45°.

The flange was pre-cured, cut to size, machined with a 25° taper along the edges and co-bonded with the uncured skin using one ply of grade 5, FM300 adhesive film. The averaged ply thickness obtained from specimen thickness measurements and micrographs was 0.148 mm for the tape, 0.212 mm for the fabric and 0.178 mm for the adhesive.

EXPERIMENTAL PROCEDURE

Quasi-static tension tests were performed in a servohydraulic load frame in displacement control at 0.4 mm/min. The specimens were mounted in hydraulic grips with a gage length of 101.6 mm. A damage onset load was determined at which a small initial load drop was observed prior to flange debonding. The value of the damage onset load was averaged from five tests and determined to be 17.8 kN which was later designated as $P_{100\%}$.

Fatigue tests were performed at a cyclic frequency of 5 Hz, an R-ratio of 0.1 and load levels corresponding to 70%, 60%, 50% and 40% of the quasi-static damage onset load. Three tests were performed at 70% and 50% and four tests were performed at 60% and 40%. The damage was monitored using a Questar digital microscope on one edge and an optical travelling microscope on the other edge. The specimen edges were painted in white to make the cracks and delaminations more visible. Damage was documented based on location at each of the four corners identified in Figure 1. The number of cycles at which the first matrix crack appeared was recorded as well as the number of cycles to delamination onset.

MICROSCOPIC INVESTIGATION

Typical damage patterns observed from specimens are shown in Figure 2. Two typical micrographs are presented in Figure 3. All quasi-static and fatigue tests yielded similar damage patterns. Under quasi-static loading, failure occurred across one flange tip of the specimen only, with no clear preference for corners 1 and 2 or corners 3 and 4. In fatigue, damage initiated at both flange tips, but not at the same time.

At corners 2 and 3, a delamination (delamination B) formed in the top 45°/-45° skin ply interface, as depicted in Figure 3a. This delamination initiated at the flange tip from a matrix crack in the top 45° skin ply. In fatigue, damage first appeared at corner 2 and 3 (delamination B) for 12 of the 14 specimens. At corners 1 and 4, a delamination running in the bondline (delamination A1) initiated from a matrix crack in the adhesive pocket, as shown in Figure 3b. In some of the quasi-static cases, a second delamination (A2) was observed below the first, in the top –45°/90° skin ply interface. Delamination A2 was not observed in fatigue, because the damage was never grown to the same extent.

FINITE ELEMENT ANALYSIS

The finite element (FE) method was used to study damage initiation using a stress analysis and the potential for delamination using fracture mechanics. The schematics of the two-dimensional model of the specimen, boundary conditions, and loads applied are shown in Figure 4. ABAQUS® eight-noded quadrilateral plane stress elements were used in geometric nonlinear analyses [4].

For the model of the undamaged specimen, a refined mesh was used in the critical area of the 45° skin ply where cracking was observed during the tests as shown in the detail of Figure 5a. Based upon examination of the tested specimen, the critical damaged was assumed to start at corners 2 and 3 in the form of a matrix crack in the top 45° skin ply and develop into a delamination, as shown in Figure 5b.

Earlier investigations [2, 3] indicated that the maximum ply principal transverse tensile stress, σ_{tt}, normal to the fiber direction may cause the initial failure in the form of matrix cracks once the transverse tensile strength of the composite material is exceeded. The computed maximum principal tensile stress distribution in the top 45º skin ply is plotted in the immediate vicinity of the flange tip in Figure 6. First matrix cracking was observed at locations where peak stresses were calculated.

A fracture mechanics approach was used to investigate delamination onset once the initial crack had formed. The Virtual Crack Closure Technique (VCCT) was used to calculate the mode I and II components of the strain energy release rates for the modeled delamination [5]. The total energy release rates computed for a delamination growing between the skin top 45º and -45º plies is plotted in Figure 7.

MATRIX CRACKING ONSET FATIGUE LIFE PREDICTION

Matrix cracking was the first damage mechanism to occur in the specimen, followed by delamination. In order to predict the onset of matrix cracking the following steps were taken.

- In Figure 8, the relationship between the externally applied tensile load, P, and the principal transverse tensile stresses, σ_{tt}, was determined by plotting the load versus the peak stress from Figure 6. To account for residual stresses after cooldown and moisture absorption, a simple analysis was performed using classical laminate theory. The results were superposed with the transverse tensile stresses obtained from finite element analysis. The resulting plot was also included in Figure 8.
- A matrix cracking onset fatigue life characterization curve was generated through three-point bending tests of 90° lamina. The transverse tensile stress σ_{ttmax}, (where "max" refers to the maximum stress resulting from the sinusoidal cyclic load applied) was plotted versus the number of cycles to failure, N, as shown in Figure 9. The fatigue life curve was obtained by curve fit of the mean life data. Additionally, scatter was addressed by constructing curves with plus and minus one standard deviation which were included in Figure 9.
- Once these calculations and characterizations were available, it was possible to determine for an arbitrary maximum cyclic load, (P_i in Figure 8), the maximum transverse tensile stress (σ_i in Figure 8) as well as the associated fatigue life (N_i in Figure 9). Plotting the relationship between the externally applied load, P, and the fatigue life, N, yielded the prediction onset curve as shown in Figure 10. This procedure was repeated using the curves with plus and minus one standard deviation in Figure 9 to obtain the set of curves in Figure 10. The prediction for matrix cracking onset in the skin/stiffener specimens is in good agreement with measured P-N data from the fatigue tests which were included in Figure 10 for verification.

DELAMINATION ONSET FATIGUE LIFE PREDICTION

Delaminations originated from the matrix cracks as shown in Figures 2 and 3. Delamination onset life was determined using computed mixed mode energy release rates at the delamination front (see Figure 7) and mixed-mode fracture toughness data for the material [6], as follows:

- The relationship between the externally applied load, P, and the total energy release rate, G_T, was determined by plotting P versus G_T at delamination onset (Δa=0.05 mm) from Figure 7 as shown in Figure 11 for several load cases and fitting a curve to theses results. Additionally, the corresponding mixed-mode ratio, R, was calculated at each load step and the results were also curve fit and plotted in Figure 11. Due to a minimal variation in the mixed mode ratio, an average constant $R=G_{II}/G_T=0.18$ was assumed for the following step.
- A failure surface relating the total energy release rate, G_{max}, to the mixed mode ratio, G_{II}/G_T, and the number of cycles to delamination onset, N, is given in reference 6. From these data, a fatigue life curve (shown in Figure 12) was constructed for R=0.18, which corresponds to the calculated average mixed mode ratio from above.
- With this information available, for an arbitrary maximum cyclic load, P_i, the total energy release rate, G_i, and the corresponding mixed mode ratio, R_i, were determined as illustrated in Figure 11. The associated fatigue life, N_i, was obtained as shown in Figure 12. Plotting the relationship between the externally applied load, P, and the fatigue life, N, yielded the prediction onset curve as shown in Figure 13. The prediction for delamination onset is in good agreement with measured P-N data from the fatigue tests, corresponding to the total life to delamination onset minus the life to matrix cracking onset in Figure 10. These data were included in Figure 13 for verification.

CONCLUDING REMARKS

A bonded composite skin/stringer specimen was used to verify a methodology for determining the fatigue life based on matrix cracking and delamination fatigue onset characterization data and geometric nonlinear finite element analyses. The predicted onset of both matrix cracking and delamination was in good agreement with test data.

REFERENCES

[1] Minguet, P.J. and O'Brien, T.K., "Analysis of Test Methods for Characterizing Skin/Stringer Debonding Failures in Reinforced Composite Panels", *Composite Materials: Testing and Design, Twelfth Volume*, ASTM STP 1274, August 1996, pp. 105-124.

[2] Cvitkovich, M. K., O'Brien, T. K., and Minguet, P. J., "Fatigue Debonding Characterization in Composite Skin/Stringer Configurations," *Composite Materials: Fatigue and Fracture, Seventh Volume, ASTM STP 1330*, 1998, pp. 97-121.

[3] Krueger, R., Cvitkovich, M. K., O'Brien, T.K. and Minguet, P.J., "Testing and Analysis of Composite Skin/Stringer Debonding Under Multi-Axial Loading," NASA TM-1999-209097, ARL-MR-439, February 1999.

[4] ABAQUS/Standard, "User's Manual, Volume II," Version 5.6, 1996.

[5] Raju, I.S., "Calculation Of Strain-Energy Release Rates With Higher Order And Singular Finite Elements", *Eng. Fracture Mech.*, 28, 1987, pp. 251-274.

[6] Hansen, P. and Martin, R.H., "DCB, 4ENF and MMB Delamination Characterization of S2/8552 and IM7/8552," Presented at the 15th Annual Technical Conference on Composite Materials, American Society for Composites – College Station, Texas, September, 2000.

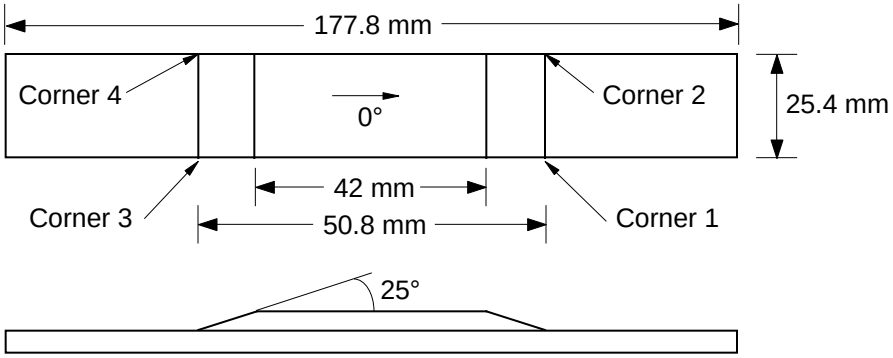

Figure 1. Specimen configuration.

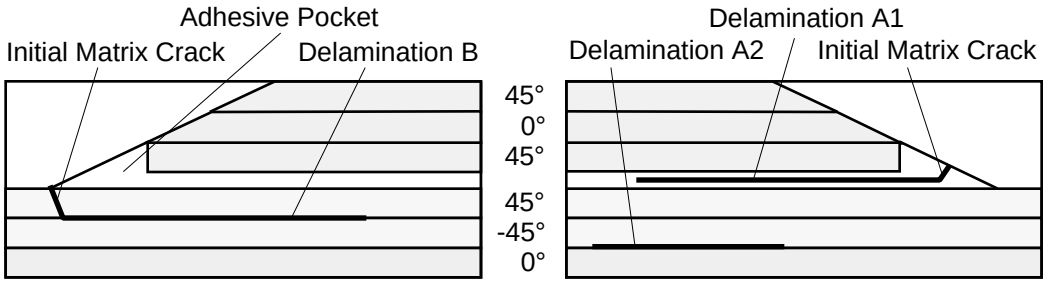

(a) Corners 2 and 3 (b) Corners 1 and 4

Figure 2. Typical damage patterns.

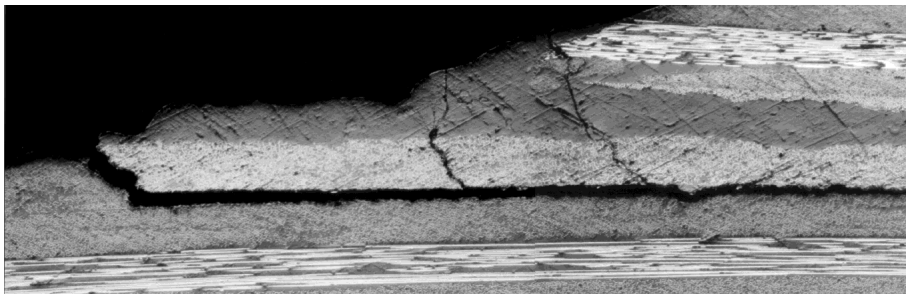

(a) Delamination B in the 45°/-45° skin ply interface at corner 3

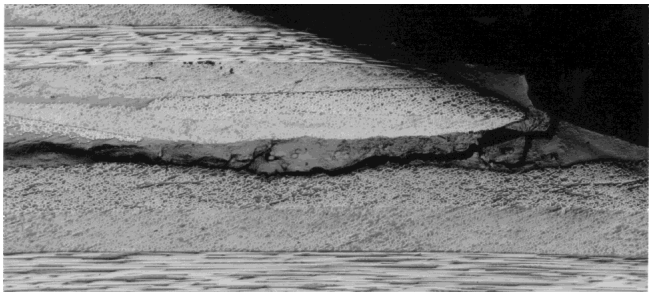

(b) Delamination A1 at the bondline at corner 1

Figure 3. Micrograph of the edge of a failed specimen.

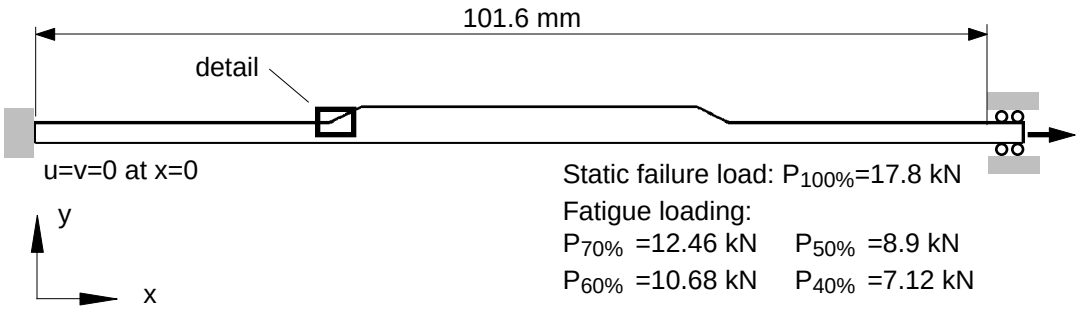

Figure 4. Loads and boundary conditions.

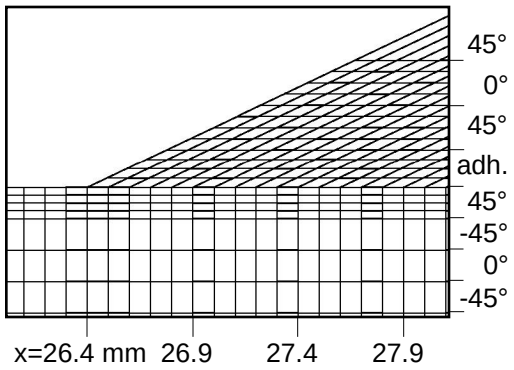

(a) Detail of undamaged specimen

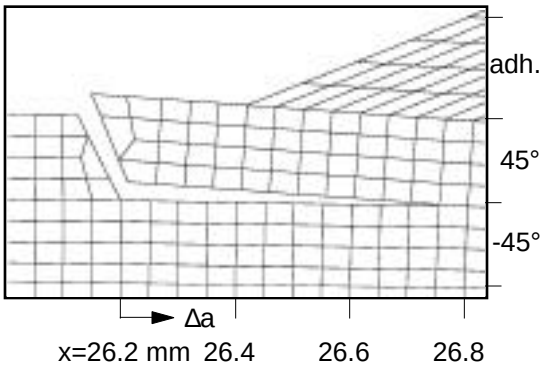

(b) Detail of damaged specimen

Figure 5. FE mesh around flange tip region.

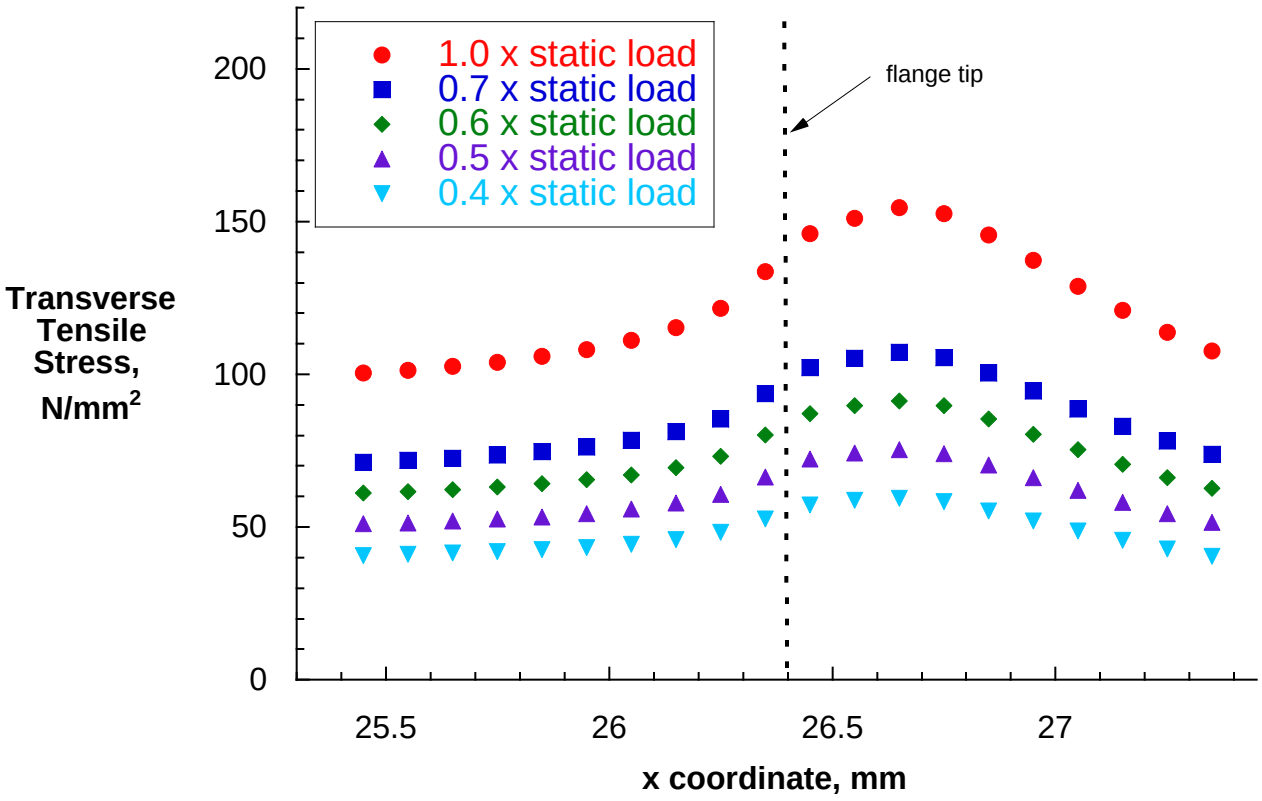

Figure 6. Computed transverse tensile stress in top 45° skin ply.

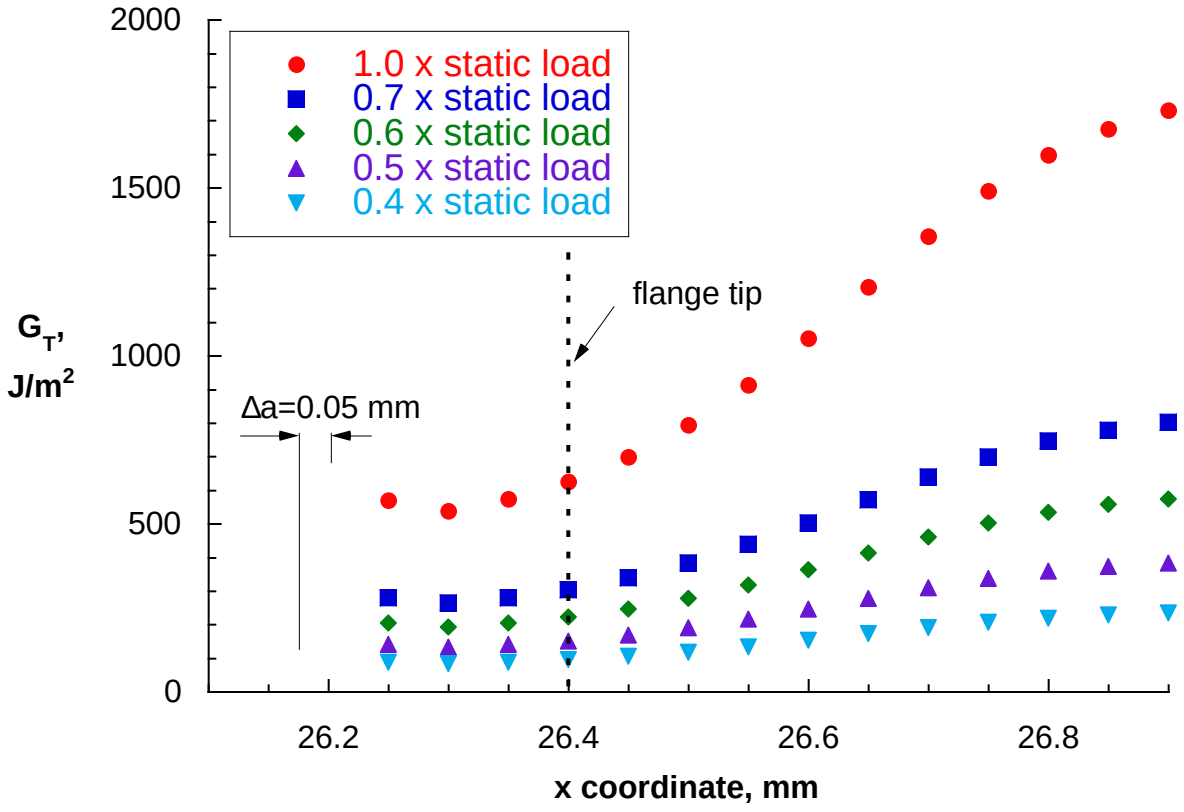

Figure 7. Computed total energy release rate for delamination in 45°/-45° interface.

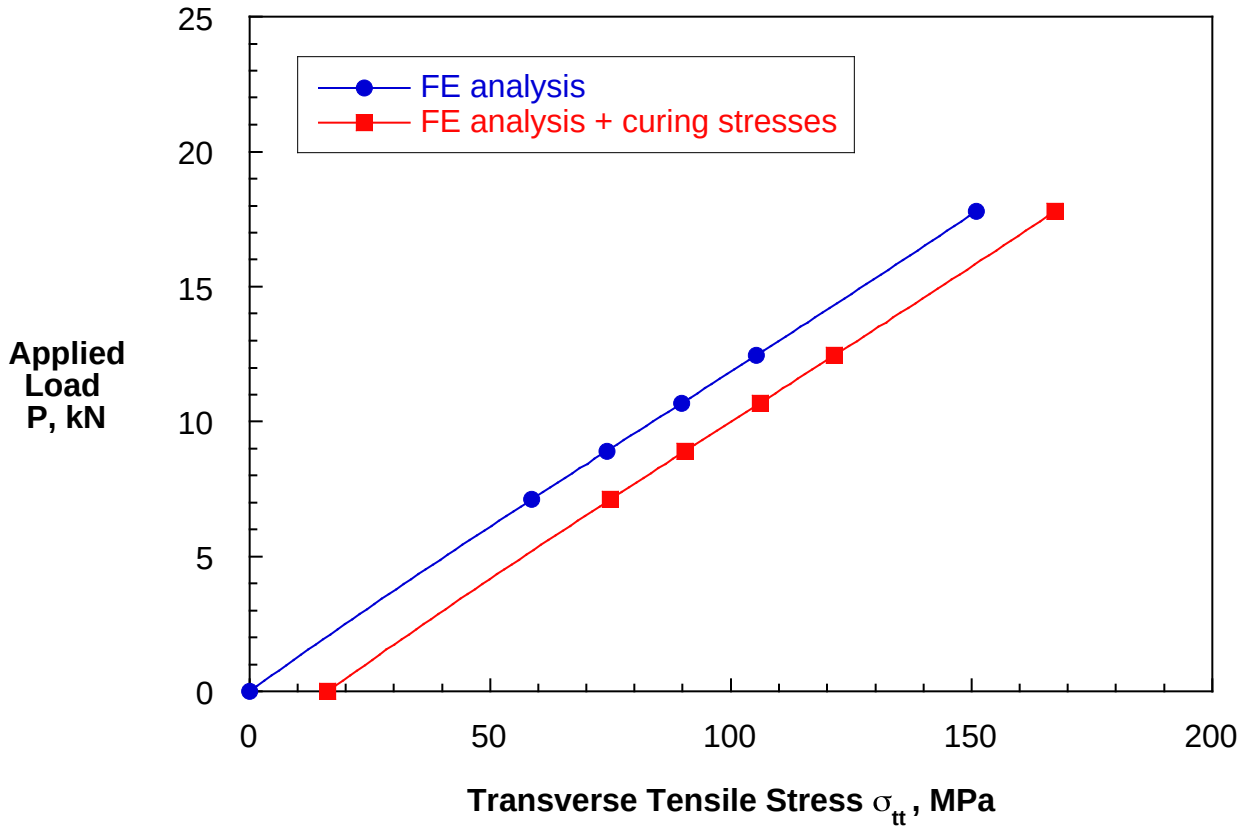

Figure 8. External load plotted versus calculated ply transverse tensile stress.

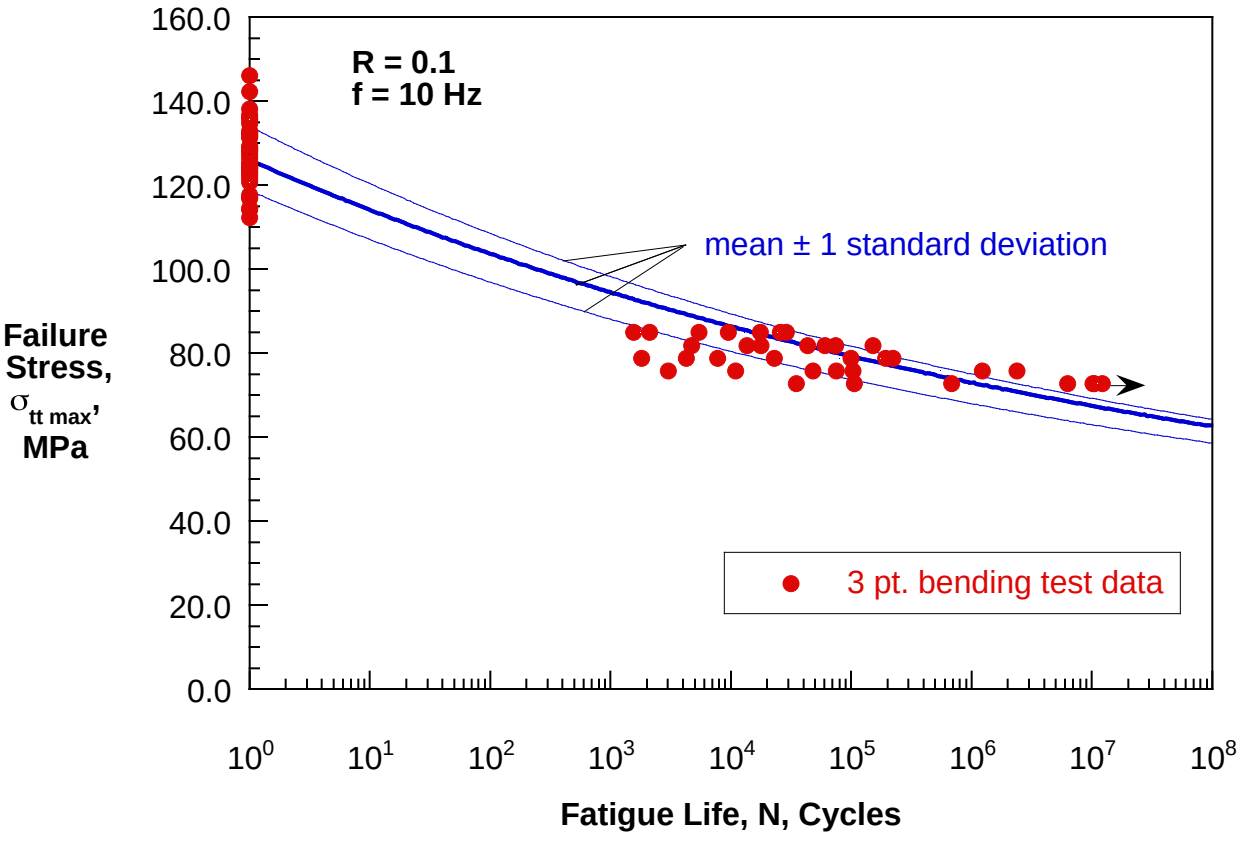

Figure 9. Fatigue life characterization data for onset matrix cracking.

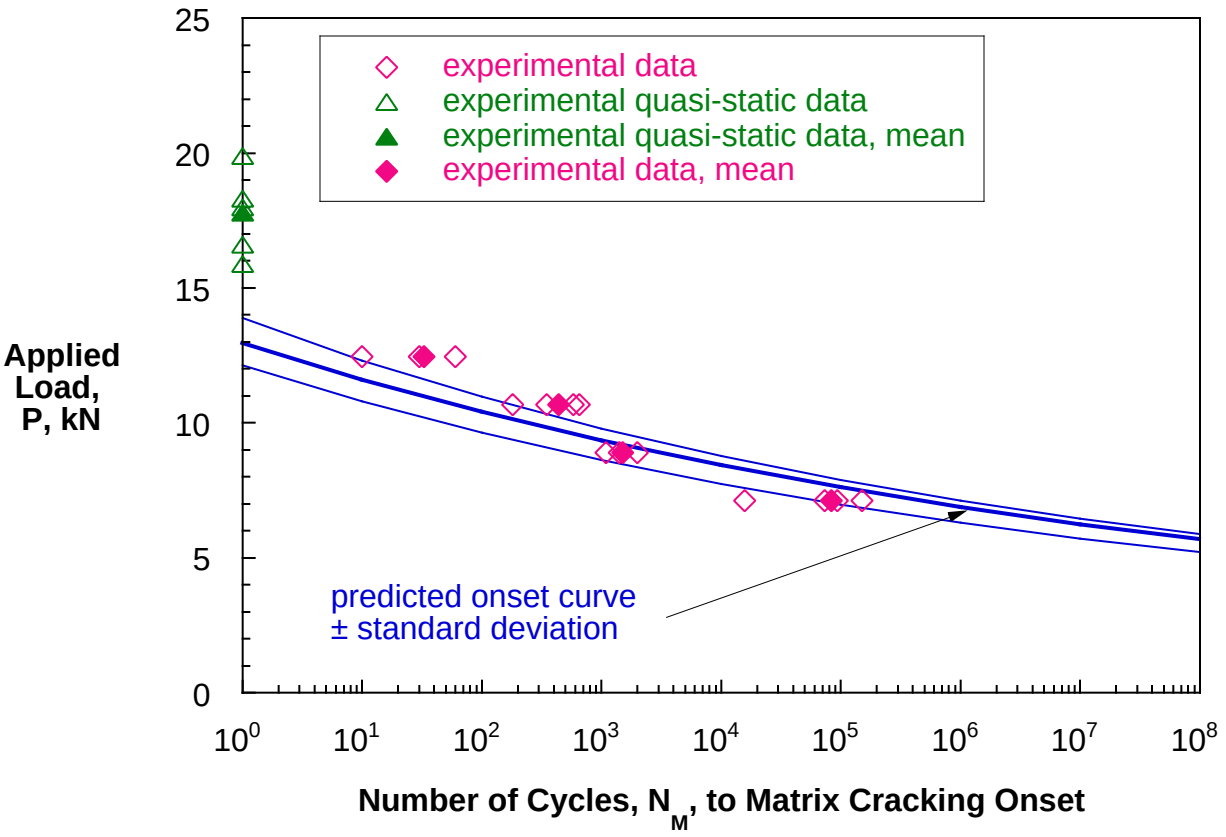

Figure 10. Comparison of matrix cracking onset prediction and experimental results.

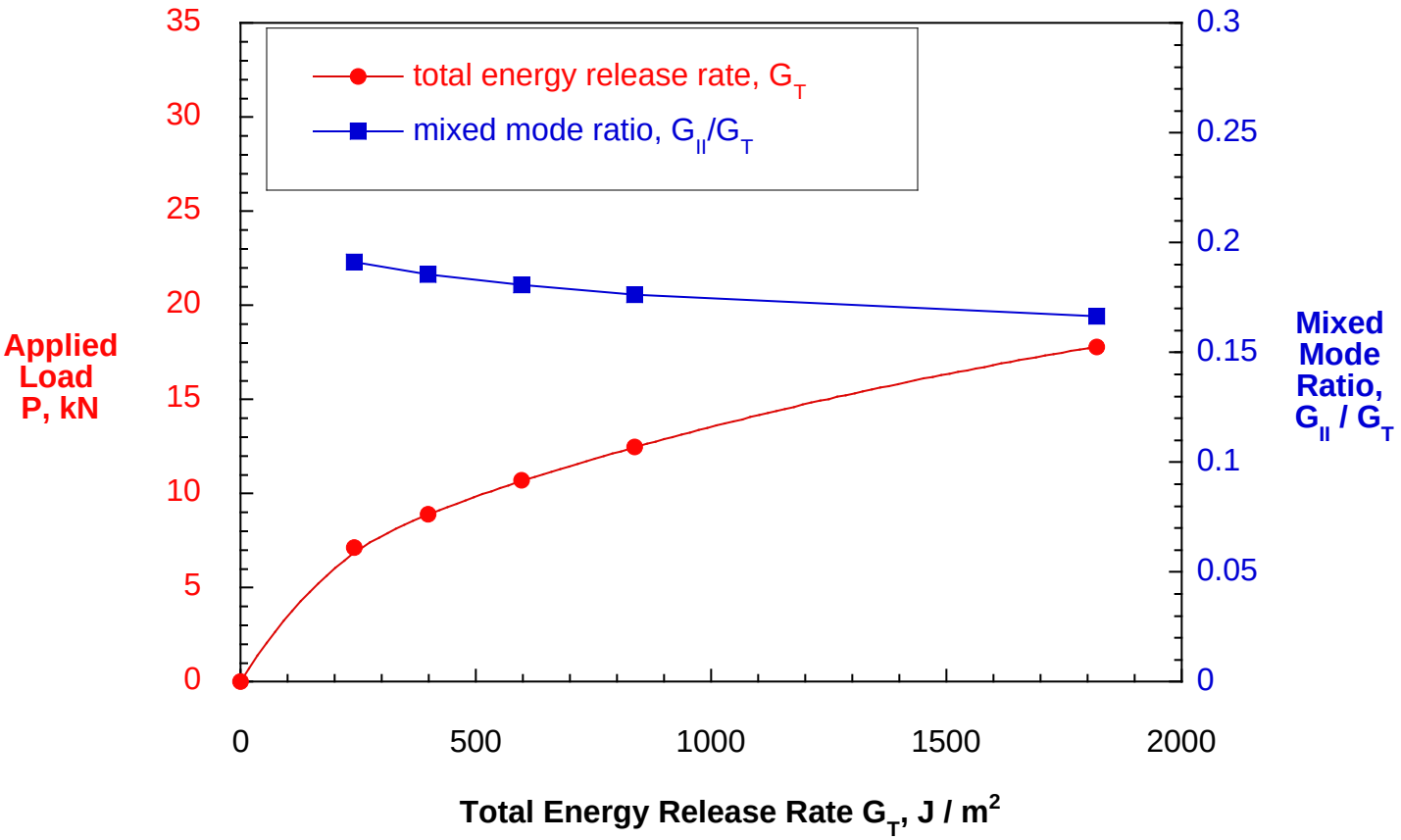

Figure 11. External load and mixed mode ratio plotted versus calculated G_T.

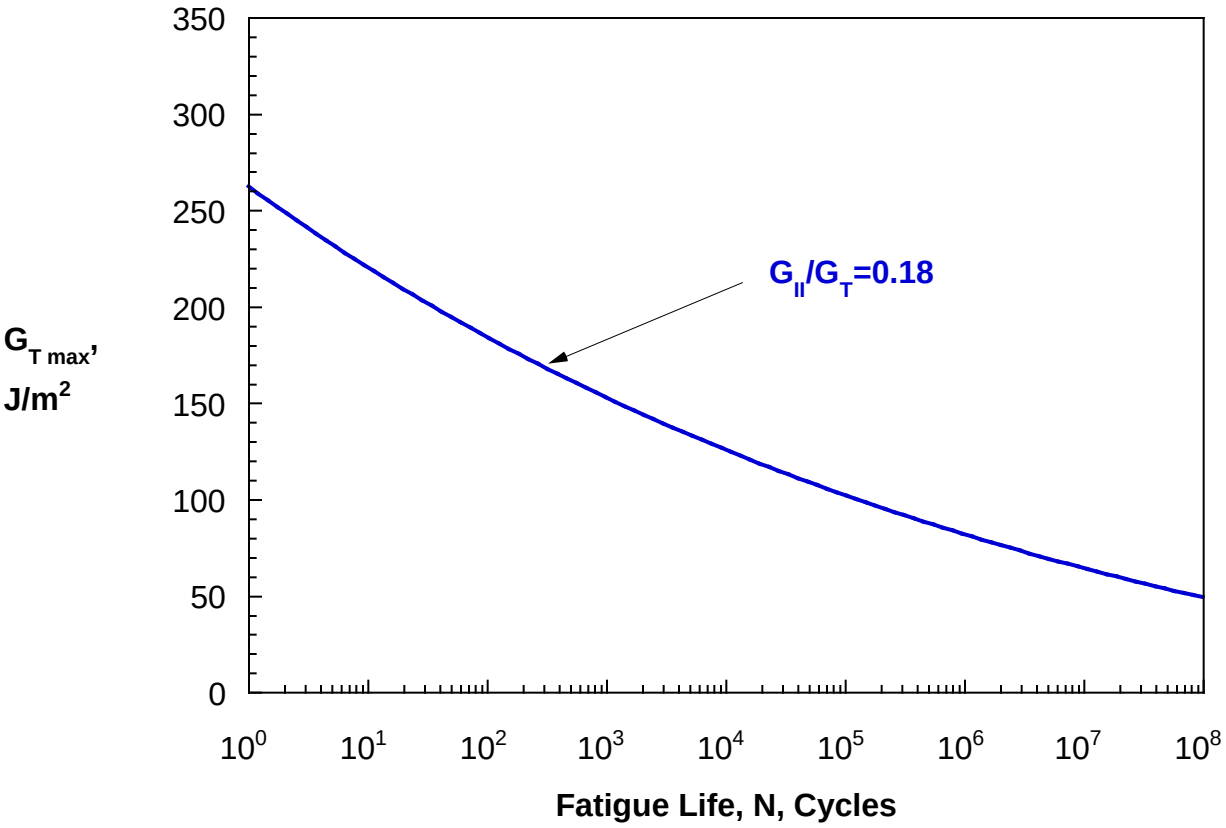

Figure 12. Delamination onset curve for constant mixed mode ratio R.

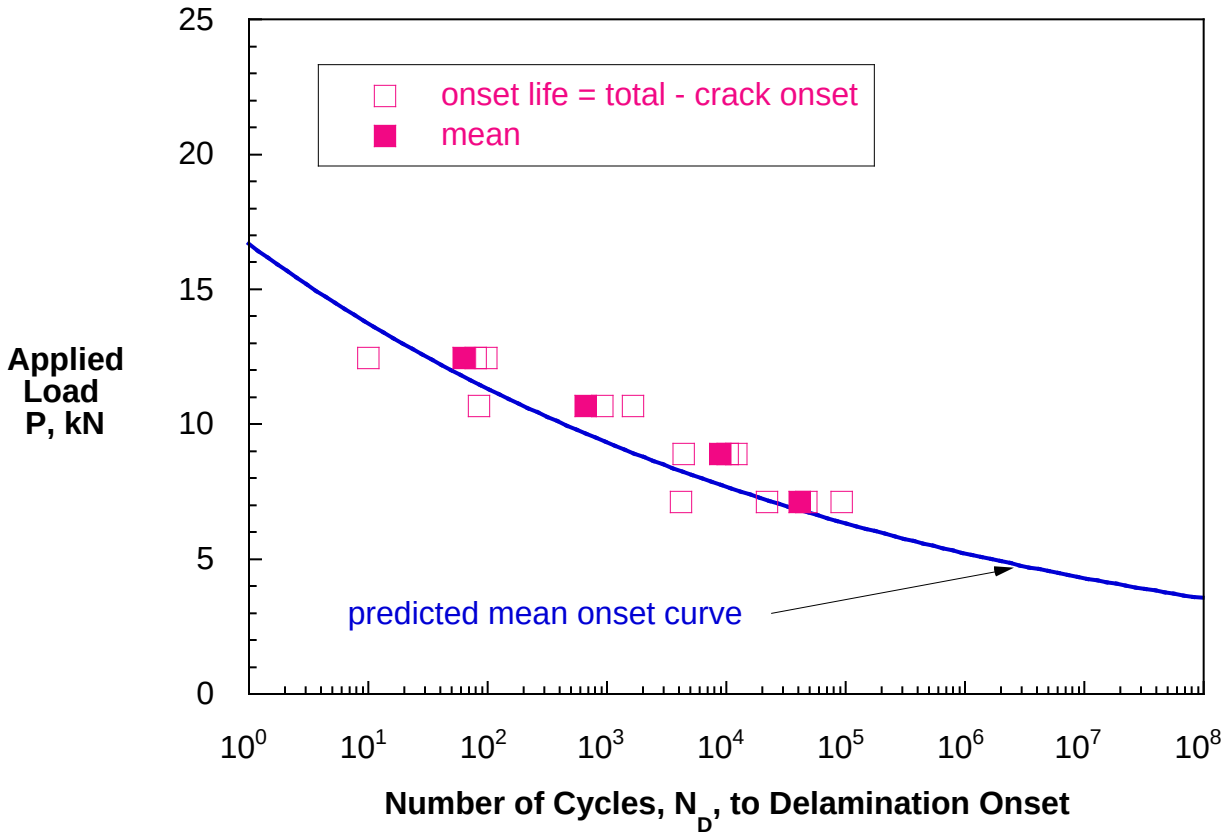

Figure 13. Comparison of delamination onset prediction and experimental results.